

THE RESEARCH OF DISCONTINUOUS GALERKIN P-MULTIGRID SOLVER

Yongheng Guo, Yong Yang & Zhijian Duan

National Key Laboratory of Science and Technology on Aerodynamic Design and Research, School of Aeronautics, Northwestern Polytechnical University, Xi'an, China

Keywords: normal orthogonal basis; p-multigrid; discontinuous Galerkin

Abstract

With unstructured elements as basic element and normal orthogonal basis as test functions, a p-multigrid solution strategy is developed for discontinuous Galerkin discretizations of the two-dimensional Euler equations. This solver is used to compute transonic flow over the airfoil NACA0012 and RAE2822. The numerical flux of Euler equations are calculated by using Roe scheme. Along the direction of time, an explicit Runge-Kutta scheme is applied for the p level (i.e. the higher order accuracy), while an implicit scheme is applied for the p-1 level (i.e. the lower order accuracy). The performance of the solver in term of convergence efficiency is investigated. Compared with the single grid (SG) solver, the p-multigrid (MG) solver is found to deliver nearly optimal convergence rate. At last, some reason of the acceleration about it is analyzed.

1 Background

In recent years, with the aviation-astronautics science and technology rapid development, there have many new requirements to computational fluid dynamics (CFD) methods, especially in aspect of enhancing the convergence rate and accuracy. However, many of the traditional CFD methods have been very difficult to meet the need. So scientists and engineers have conducted a long-term in-depth study, especially since the 1990s, the Runge-Kutta discontinuous Galerkin (RKDG) method has been given by Cockburn and Chi-Wang Shu as the representative [1], which has become a hot issue, and reached a high-precision approach to many problems. For

discontinuous Galerkin (DG) formulations, the element-to-element coupling exists only through the flux at the shared boundaries between elements, therefore, the shockwave is easier to capture using RKDG method to solve aerodynamics problems.

However, to improve accuracy and enhance the convergence rate is often a conflict, DG method is no exception. To enhance the precision approach based on the need to improve the function of the space dimension, each corresponding to the number of degrees of freedom have increased and each unit corresponds to the number of degrees of freedom have increased. On the other hand, in order to meet the convergence requirements of the discontinuous Galerkin format, a large number of numerical integration need to be calculated on the cell [2]. All this has greatly increased the CPU time, to a certain extent, limited the application of DG method.

In order to resolve this contradiction, this article applied multi-grid technology to DG method format. Different from the traditional multi-grid algorithm design, this paper established the p-Multigrid algorithm which needn't adjust the physical scale of the grid, but through adjusted basis function of the space dimension to achieve the method directly.

The organization of this paper is as follows. The governing equations to be solved are described in Section 2. Section 3 describes the spatial discretization used in this work, including the implicit solution for the low level of the multigrid solver. Section 4 describes the initial and boundary conditions. In Section 5, the operators for the multigrid solver are constructed. Section 6 describes the two level multi-grid solvers and in Section 7 the

computational result is showed, including some analysis. Finally, Section 8 summarizes the conclusions of this paper.

2 Governing Equations

The conservative form of the compressible Euler equations describing the conservation of mass, momentum and total energy are given in vectorial form

$$\frac{\partial Q}{\partial t} + \frac{\partial F(Q)}{\partial x} + \frac{\partial G(Q)}{\partial y} = 0 \quad (1)$$

The expression of each vector is as follows:

$$Q = (\rho \quad \rho u \quad \rho v \quad E)^T,$$

$$F = (\rho u \quad \rho u^2 + p \quad \rho uv \quad u(E + p))^T \quad (2)$$

$$G = (\rho v \quad \rho uv \quad \rho v^2 + p \quad v(E + p))^T$$

where ρ is the fluid density, (u, v) are the fluid velocity Cartesian components, p is the pressure and E is the total energy per unit volume respectively. For an ideal gas, the equation of state related the total energy to pressure by:

$$E = \frac{p}{\gamma - 1} + \frac{1}{2} \rho (u^2 + v^2) \quad (3)$$

where $\gamma = 1.4$ is the ratio of specific heats.

3 Spatial Discretization

First, the computational domain Ω is divided into a set of non-overlapping unstructured elements $\Omega = \bigcup_{i=1}^N \Omega_i$. In this article, a set of triangle elements are obtained. The partial solution space of DGM is defined as a set of the multinomial with different exponent number, which is recorded as $V_h(k)$. On each unit, the finite element solution is expressed as:

$$Q_h(x, y, t) = \sum_{j=1}^n Q_j(t) \varphi_j(x, y) \quad (4)$$

where n is the dimension number of the partial solution space, and φ_j ($j = 1, 2, \dots, n$) is the basis functions. According to variational principle, it

is necessary to suppose the test function space to be the same with the solution space^[3]. In the following process, inner product operation is made in such scheme :

$$\iint_{\Omega_i} \varphi_j \left(\frac{\partial Q}{\partial t} + \frac{\partial F}{\partial x} + \frac{\partial G}{\partial y} \right) dV = 0 \quad (5)$$

Let (n_x, n_y) be the normal vector in the boundary of the current element, the direction of which is outward, and define the flux vector as:

$$\bar{H} = F \cdot \bar{i} + G \cdot \bar{j} \quad (6)$$

According to Green's theorem, the weak form of equations (4), namely, the discontinuous Galerkin equation is obtained:

$$\begin{aligned} \frac{d}{dt} \iint_{\Omega_i} \varphi_j Q_h dx dy - \iint_{\Omega_i} \nabla \varphi_j \cdot \bar{H} dx dy \\ + \oint_{\partial \Omega_i} \varphi_j \bar{H} \cdot \bar{n} ds = 0 \end{aligned} \quad (7)$$

where $\bar{H} \cdot \bar{n}$ is the numerical flux between the current and the neighboring cells. Here, Roe's upwind scheme is applied^[4]. By means of linear substitution, each element is mapped into an isosceles triangle under the computation coordinate system, namely,

$$D := \{(\xi, \eta) | 0 \leq \eta \leq 1 - \xi, 0 \leq \xi \leq 1\} \quad (8)$$

According to the Gram-Schmidt principle^[5], the following standard orthogonal basis is established:

$$e_1 = \sqrt{2},$$

$$e_2 = 6\xi - 2, \quad (9)$$

$$e_3 = 2\sqrt{3}(2\eta - 1 + \xi), \dots$$

and the basis functions have following nature:

$$\iint_D \varphi_i \varphi_j d\xi d\eta = \begin{cases} 1, & i = j \\ 0, & i \neq j \end{cases} \quad (20)$$

For simplicity, e_1, e_2, e_3 are taken as the basis functions for the p level (i.e. the higher order accuracy) discretization. Let $\varphi_j(x, y) = e_j(\xi, \eta)$ ($j = 1, 2, 3$), the mass matrix

and its inverse correspond to the discontinuous Galerkin equation degenerated to diagonal matrix, respectively. Thus, it is clear that the computational process obtains an obvious simplification. Consider the triangle element, Gauss integral is applied to replace the one in element interior and boundary. Similar with the situation in FVM, local time steps is used on each element. Unified a four-order explicit Runge-Kutta scheme, the stability of the algorithm is enhanced. Such is the discretization of the p level. Finally, the steady state of the flowfield is obtained.

Consider the discretization for the p-1level (i.e. the lower order accuracy), the constant basis is taken as the test function:

$$e = 1, Q_h = Q_i e = Q_i \quad (31)$$

In order to accelerate the convergence rate, an implicit discretization is used on this level:

$$V \frac{\Delta Q_i}{\Delta t} + \sum_{j=1}^3 \bar{H}(Q_i^{n+1}, Q_j^{n+1}) \cdot \bar{n} S_{ij} = 0 \quad (42)$$

where, V is the area of the element, and S_{ij} is the length of each boundary. $\Delta Q_i = Q_i^{n+1} - Q_i^n$. For simplicity, Taylor's law is applied:

$$\bar{H}_{ij}^{n+1} \cdot \bar{n} = \bar{H}_{ij}^n \cdot \bar{n} + A_i^+(Q_i^n) \Delta Q_i + A_j^-(Q_j^n) \Delta Q_j \quad (53)$$

Where

$$A^\pm := \frac{1}{2}(A \pm \lambda I) \quad (64)$$

Jacobian Matrix is:

$$A := \frac{\partial H(Q)}{\partial Q} = \frac{\partial F(Q)}{\partial Q} \cdot n_x + \frac{\partial G(Q)}{\partial Q} \cdot n_y \quad (75)$$

And its spectrum radius is:

$$\lambda = |u \cdot n_x + v \cdot n_y| + a \quad (86)$$

where a is local sound speed.

Consider the current element, it is obvious that:

$$A(Q_i) \Delta Q_i \cdot S_{ij} = 0 \quad (97)$$

So, for each element, an implicit liner system is obtained as following:

$$\left(\frac{V}{\Delta t} + \frac{1}{2} \sum_{j=1}^3 \lambda_j(Q_i^n) \cdot S_{ij} \right) \Delta Q_i + \sum_{j=1}^3 A^-(Q_j^n) \cdot S_{ij} \Delta Q_j + \sum_{j=1}^3 \tilde{H}_j^n(Q_i^n, Q_j^n) \cdot S_{ij} = 0 \quad (108)$$

4. Initial and Boundary Conditions

Consider the flowfield of the airfoil, in the initialization, the state of each element is consistent with the one on the far field. For discontinuous Galerkin equation, it is necessary to initialize the coordinate of the finite element solution, namely the time-dependent variables in the partial space, i.e. the finite element solution needs to approach the initialization of the flow field squarely. Furthermore, the streamline must be consistent with the wall.

5. Operator Definition

Consider the two terms of discretized system above, both of them can be given by^[6]:

$$R^p(Q^p) = f^p \quad (119)$$

where $R^p(Q^p)$ is the associated nonlinear system, and f^p is a source term(zero for the fine-level problem). The discrete residual r^p is defined as:

$$r^p = f^p - R^p(Q^p) \quad (20)$$

In order to define the residual restriction operator, the basis function for p-1 level is expressed by the one for p level^[7]:

$$\Phi_i^{p-1} = \sum_j \alpha_{ij}^{p-1} \Phi_j^p \quad (21)$$

Here,

$$\Phi_1^{p-1} = 1, \quad (22)$$

$$\Phi_1^p = e_1 = \sqrt{2},$$

$$\begin{aligned}\Phi_2^p &= e_2 = 6\xi - 2 \\ \Phi_3^p &= e_3 = 2\sqrt{3}(\xi + 2\eta - 1)\end{aligned}$$

In the linear space generated by the basis functions, it is obvious that the vector group $\{\Phi_1^p, \Phi_2^p, \Phi_3^p\}$ is linear independence and the vector group $\{\Phi_1^{p-1}, \Phi_1^p, \Phi_2^p, \Phi_3^p\}$ is linear dependence. According to the knowledge in advanced algebra, the expression form about formula (22) is only. The coefficient α_{ij}^{p-1} can be easily obtained: $\alpha_{11}^{p-1} = \frac{1}{\sqrt{2}}$, $\alpha_{12}^{p-1} = \alpha_{13}^{p-1} = 0$, so the residual restriction operator, I_p^{p-1} , is obtained as:

$$I_p^{p-1} = (\alpha_{ij}^{p-1}) = \left(\frac{1}{\sqrt{2}}, 0, 0\right) \quad (23)$$

In the computational domain, D , the state variables Q^{p-1} is the best square approaches of Q^p :

$$\iint_D \Phi_1^{p-1} Q_h^{p-1} d\xi d\eta = \iint_D \Phi_1 Q_h^p d\xi d\eta \quad (24)$$

where $Q_h^{p-1} = Q_1^{p-1} \cdot \Phi_1^{p-1}$,

$$Q_h^p = Q_1^p \Phi_1^p + Q_2^p \Phi_2^p + Q_3^p \Phi_3^p$$

After the simplification of equation(24), it is obtained that

$$Q_1^{p-1} = Q_1^p \cdot \sqrt{2} \quad (25)$$

So, the state restriction operator, \tilde{I}_p^{p-1} , is

$$\tilde{I}_p^{p-1} = (\sqrt{2}, 0, 0) \quad (26)$$

At last, according to physics significance, the state prolongation operator can be easily obtained as:

$$\tilde{I}_{p-1}^p = \left(\frac{1}{\sqrt{2}}, 0, 0\right)^T \quad (27)$$

Now, it is obvious that most elements of the restriction and prolongation operator are equal to zero as a result of the normal orthogonal basis

being used. In practice, operators with this nature make the computational process simple obviously.

6. Two Level Multigrid Solver

Now, a two level multigrid solver is designed as the following four steps:

Step 1:

On the p level, Runge-Kutta scheme is applied along the direction of time;

Step 2:

Restrict the state and residual vectors from the p level to the $p-1$ level, i.e.

$$Q_0^{p-1} = \tilde{I}_p^{p-1} Q^p, \quad r^{p-1} = I_p^{p-1} r^p \quad (28)$$

Step 3:

Equations are obtained on the $p-1$ level as follows

$$R^{p-1}(Q^p) = R^{p-1}(Q_0^{p-1}) + r^{p-1} \quad (29)$$

According to Taylor's law,

$$\begin{aligned}R^{p-1}(Q^{p-1}) &\approx R^{p-1}(Q_0^{p-1}) \\ &+ \left. \frac{\partial R}{\partial Q} \right|_{Q=Q_0^{p-1}} \cdot (Q^{p-1} - Q_0^{p-1})\end{aligned} \quad (30)$$

Further, a simplification of equations (29) are obtained

$$\left. \frac{\partial R}{\partial Q} \right|_{Q=Q_0^{p-1}} \cdot (Q^{p-1} - Q_0^{p-1}) = r^{p-1} \quad (31)$$

It is known that the large-scale sparse linear system can be solved by LUSGS algorithm easily.

Step 4:

Prolongate the $p-1$ level error and correct the p level state:

$$Q^p = Q^p + I_{p-1}^p \Delta Q^{p-1} \quad (32)$$

Now, a V-circle of the two level p -multigrid solver is completed. After several V-circle, the flowfield of the airfoil NACA0012 can be computed rapidly by this solver.

7. Computational Result and Analysis

Around the airfoil NACA0012 and RAE2822, unstructured elements are generated, and the grid becomes highly concentrated approach to the wall, as Figures.1-2 shown below:

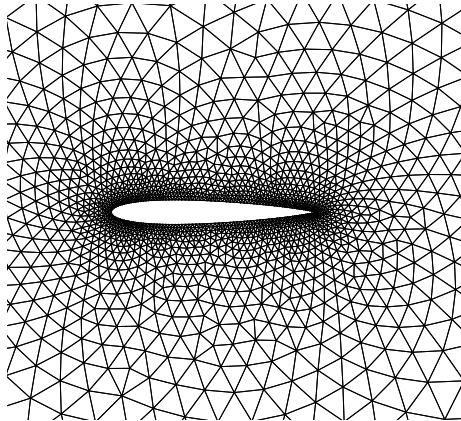


Fig 1. Grid for the computational domain (NACA0012)

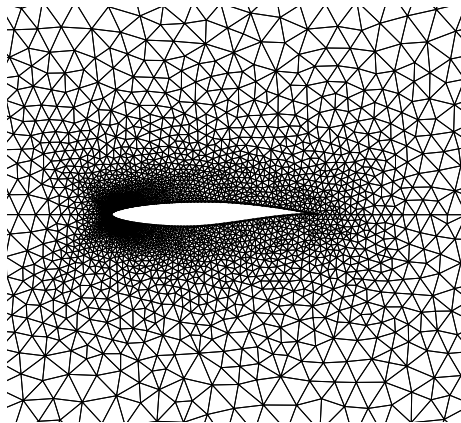


Fig 2. Grid for the computational domain (RAE2822)

Consider the transonic flow over the airfoil NACA0012. Let $Ma_\infty = 0.8$, $\alpha = 1.25^\circ$ be the boundary condition in the far field. Then, the flow field is computed by single grid (SG) and p multigrid (MG) solver respectively.

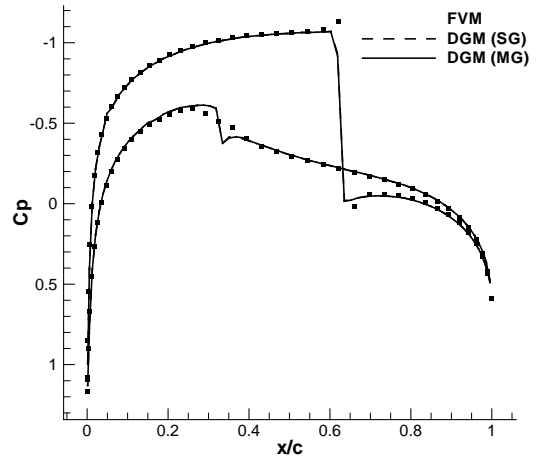


Fig 3. Distribution of pressure coefficient(NACA0012)

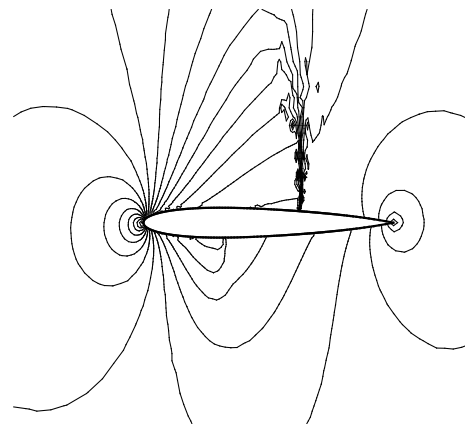


Fig 4. Distribution of isopiestic (NACA0012)

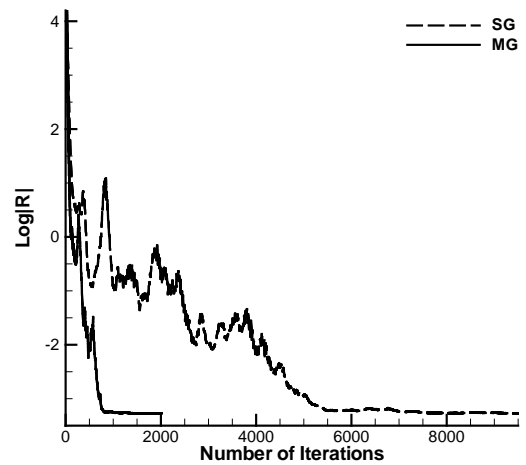


Fig5. The L_2 norm of the residual vs. number of iterations (NACA0012)

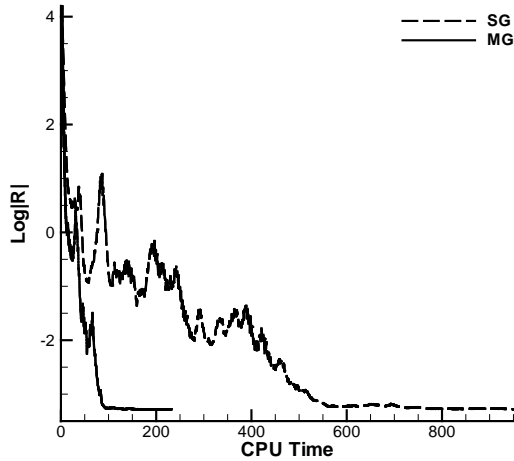


Fig6. The L_2 norm of the residual vs. CPU times (NACA0012)

Figure 3 shows the distribution of pressure coefficient around the airfoil. It is obvious that the result obtained by MG solver is completely consistent with the one obtained by SG solver. Particularly, it is difficult to separate the curve near the shockwave computed by MG solver from the one computed by SG solver. So, it is believed that the precision of MG solver is not reduced compared to SG solver. Furthermore, not only the strong shock wave but also the weak one is captured, which is more splendid than the performance of FVM. Figure 4 shows the Distribution of isopiestic around the airfoil. Figure 5 shows the L_2 norm of the residual vs. number of iterations, and Figure 6. shows the L_2 norm of the residual vs. CPU time. Thanks to the application of p-multigrid solver, 80~90 percent iterations and CPU time is saved, approximately. Clearly, p-multigrid solver designed in this article has a positive effect on the convergence rate. It implies that the implicit scheme on the lower level of p-multigrid correct the finite element solution effectively. In the process of iteration, longer time step can be used in the implicit scheme, rather than in the explicit one. Simultaneously, the system is simplified according Taylor's law as equations (30), in which residual does not need to be calculated complicated furthermore. So, the implicit scheme plays a decisive role in the aspect of enhancing the algorithm efficiency. In order to confirm the effect of the p-multigrid method furthermore, the transonic flowfield of

the airfoil RAE2822 is simulated. Let $Ma_\infty = 0.729$, $\alpha = 2.31^\circ$ be the boundary condition in the far field, and the result is shown as Figures 7-10.

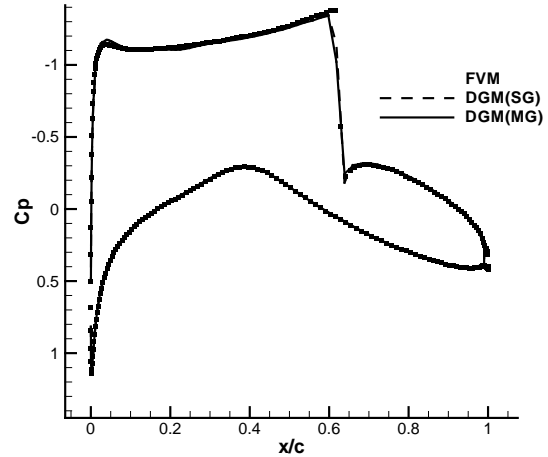


Fig 7. Distribution of pressure coefficient(RAE2822)

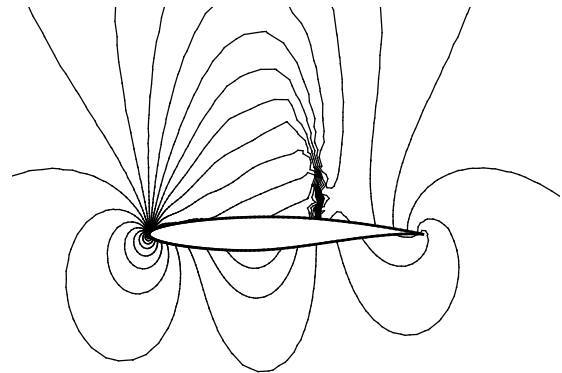


Fig 8. Distribution of isopiestic (RAE2822)

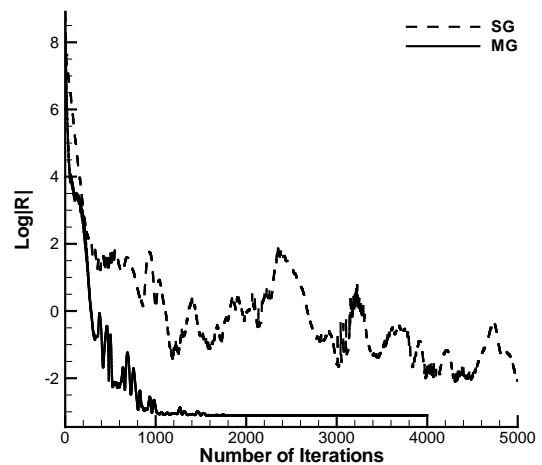


Fig9. The L_2 norm of the residual vs. number of iterations (RAE2822)

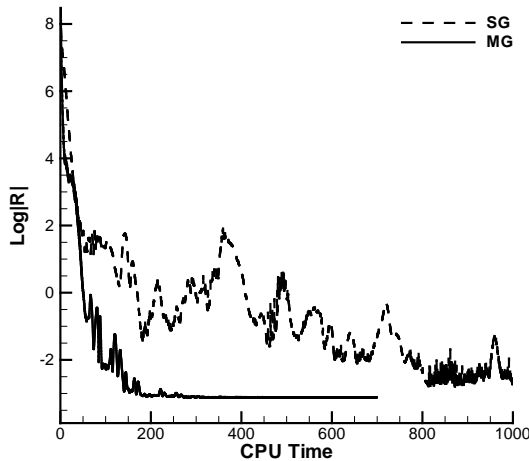


Fig10. The L_2 norm of the residual vs. CPU times
(RAE2822)

Clearly, the effect of acceleration obtains a perfect demonstration again.

8. Concluding Remarks and Work in Progress

A high-order discontinuous Galerkin discretization using normal orthogonal basis functions has been developed and implemented using a p-multigrid approach. Euler equations has been solved by this solver efficiently and the transonic flowfield is simulated perfectly. Compared with the single grid solver, a great quantity CPU time is saved. Future work will concentrate on extending the techniques to the N-S equations. In addition, implicit scheme will be applied in every level of the p-multigrid solver with the aim of raising the convergence rate and stability.

References

[1] B.Cockburn and C.W.Shu.*TVB Runge-Kutta local projection discontinuous Galerkin finite element method for scalar conservation laws II :general framework*.Math.Comp.,(52): pp 411-435,1989
 [2] Cristian R.Nastase and Dimitri J.Mavriplis , *Discontinuous Galerkin Methods Using an hp-Multigrid Solver for Inviscid Compressible Flows on Three-dimensional Unstructured Meshes*, 44th AIAA Aerospace Sciences Meeting and Exhibit,January 9-12,2006

[3] Wang Lieheng and Xu Xuejun,*The Mathematical Foundations of the Finite Element Method*.Beijing:Science Press,2004
 [5] Cheng Qixiang, Zhang Dianzhou and Wei Guoqiang, *Real Variable Function and Functional Analysis*.Beijing: Higher Education Press,2003
 [4] Roe P L.*Approximate Riemann Solver,Parameter Vectors and Different Schemes* [J].Journal of Computational Physics,43: pp357-372,1981
 [6] Liu Chaoqun, *The Application of Multigrid Method in Computational Fluid Dynamics*. Beijing: Qinghua Press,1995
 [7] Krzysztof J.Fidkowski, *A High-Order Discontinuous Galerkin Multigrid Solver for Aerodynamic Applications*, Massachusetts Institute of Technology 2004,pp 32-38

Copyright Statement

The authors confirm that they, and/or their company or organization, hold copyright on all of the original material included in this paper. The authors also confirm that they have obtained permission, from the copyright holder of any third party material included in this paper, to publish it as part of their paper. The authors confirm that they give permission, or have obtained permission from the copyright holder of this paper, for the publication and distribution of this paper as part of the ICAS2010 proceedings or as individual off-prints from the proceedings.